Nonreciprocal ballistic transport in asymmetric bands

M. H. Zou,[1] H. Geng,[1,*] R. Ma,[2] Wei Chen,[1] L. Sheng,[1,†] and D. Y. Xing[1]
[1]*National Laboratory of Solid State Microstructures, School of Physics, and Collaborative Innovation Center of Advanced Microstructures, Nanjing University, Nanjing 210093, China*
[2]*Nanjing University of Information Science and Technology, Nanjing 210044, China*

(Received 20 December 2023; revised 18 March 2024; accepted 19 March 2024; published 2 April 2024)

Nonreciprocal transport in uniform systems has attracted great research interest recently and the existing theories mainly focus on the diffusive regime. In this study, we uncover a scenario for nonreciprocal charge transport in the ballistic regime enabled by asymmetric band structures of the system. The asymmetry of the bands induces unequal Coulomb potentials within the system as the bias voltage imposed by the electrodes inverts its sign. As a result, the bands undergo different energy shifts as the current flows in opposite directions, giving rise to the nonreciprocity. Utilizing the gauge-invariant nonlinear transport theory, we show that the nonreciprocal transport predominantly originates from the second-order conductance, which violates the Onsager reciprocal relation but fulfills a generalized reciprocal relation similar to that of unidirectional magnetoresistance. The ballistic nonreciprocal transport phenomena differ from the diffusive ones by considering the internal asymmetric Coulomb potential, a factor not accounted for in diffusive cases but undeniably crucial in ballistic scenarios. Our work opens an avenue for implementing nonreciprocal transport in the ballistic regime and provides an alternative perspective for further experimental explorations for nonreciprocal transport.

DOI: 10.1103/PhysRevB.109.155302

I. INTRODUCTION

Reciprocity in charge transport reflects a symmetrical relationship between current and voltage, where the magnitude of current stays constant when the voltage has an opposite sign but the same value [1,2]. Violations of reciprocity underpin the functionality of key electronic devices like diodes and photodetectors [3,4]. Although nonreciprocal transport is commonly encountered at systems involving interfaces, such as the celebrated *p-n* junction, its implementation in uniform bulk materials has occurred more recently, driven by entirely different scenarios. A type of nonreciprocal transport, termed electric magnetochiral anisotropy (EMCA), which exhibits unidirectional magnetoresistance, was proposed in Ref. [5]. Inspired by this discovery, extensive exploration has been conducted to identify material candidates that exhibit nonreciprocal transport. Significant findings encompass chiral nanosystems [5,6], polar semiconductors [7–9], bilayer heterojunctions [10–14], and topological systems [15,16].

On the theoretical side, a variety of mechanisms have been put forward to explain nonreciprocal transport in systems with translational symmetry. Typical scenarios include asymmetric band structures [1,7], asymmetric inelastic scattering by spin clusters [17] and magnons [18], quantum metric [19,20], quantum interferences [21], and the non-Hermitian skin effect [22,23]. In these studies, various theoretical approaches have been employed, such as semiclassical transport equations [7,19,24,25] and quantum kinetic theory [26], both of which consider the nonlinear effects of an external electric field.

Here, we mainly focus on the nonreciprocal transport in the systems with asymmetric bands. The existing mechanism for this case mainly concentrates on the diffusive limit [7], and a direct extension to the ballistic limit is not feasible under the same theoretical framework.

Notably, both first-order and second-order conductivities derived in the diffusive regime diverge to infinity as the relaxation time τ approaches infinity [7], highlighting challenges in the ballistic regime. Therefore, it remains an open question whether nonreciprocal transport can be achieved in the ballistic regime. The recent application of the nonlinear Landauer formula has addressed the issue [27], yet it takes no account of the internal Coulomb potential, which results in gauge dependence as evidenced by variations in the nonlinear current with global voltage shifts. Meanwhile, a gauge-invariant nonlinear theory developed decades ago offers a more solid framework [28–30]. This approach has recently provided valuable insights, particularly in studies on nonlinear Hall effects [31,32].

In this work, we give an affirmative answer to this question by showing that nonreciprocal ballistic transport can be implemented in systems featuring asymmetric band structures with the setup depicted in Fig. 1. In this scenario, the asymmetry of the bands induces unequal Coulomb potentials $U(\Delta V)$ within the system as the bias difference $\Delta V = \mathcal{V}_{\mathrm{L}} - \mathcal{V}_{\mathrm{R}}$ between the terminals undergoes a change in sign, because the current flowing in opposite directions is carried by electrons with different densities. This leads to different energy shifts as the current flows in opposite directions. Consequently, the states occupied by electrons in the bands are situated at different levels in the original band structures without the

*genghao@nju.edu.cn
†shengli@nju.edu.cn

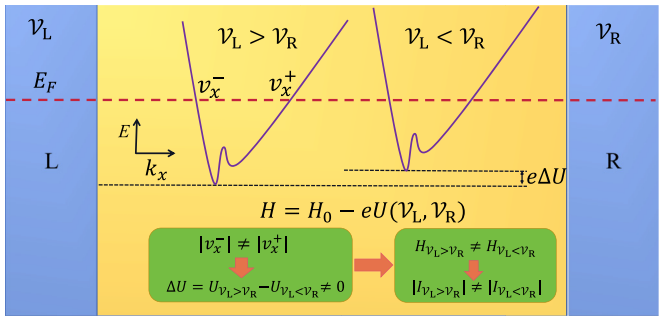

FIG. 1. The two-terminal setup for the nonlinear nonreciprocal transport system with asymmetric band structures. The terminals, depicted in blue, are designated as "L" (left) and "R" (right) with biases $\mathcal{V}_L$ and $\mathcal{V}_R$. The region in yellow represents the scattering regime. The asymmetric band structure is illustrated by the purple lines. In equilibrium, the Fermi level and the Hamiltonian are denoted by E_F and H_0, respectively. The internal screened Coulomb potential, represented as $U(\mathcal{V}_L, \mathcal{V}_R)$, correlates with the biases at the terminals. The term $v_x^{\pm}$ indicates the velocity of the right-moving (left-moving) mode around the Fermi energy. The current generated in the system, as a result of the potential difference, is expressed by $I(\mathcal{V}_L, \mathcal{V}_R)$. ΔU, the difference of Coulomb potential $U(\mathcal{V}_L, \mathcal{V}_R)$ in the cases of $\mathcal{V}_L > \mathcal{V}_R$ and $\mathcal{V}_L < \mathcal{V}_R$, makes a shift of the bottom of energy bands.

effect by Coulomb potentials, resulting in nonreciprocal transport. By utilizing the theoretical framework of gauge-invariant nonlinear quantum transport [28–30], we demonstrate the nonreciprocal ballistic transport in a two-terminal setup by showing $|I(\Delta V, B)| \neq |I(-\Delta V, B)|$, where B is the magnetic field utilized to generate band asymmetry. We further show that, although the Onsager reciprocal relation [33] breaks down here, the relation $|I(\Delta V, B)| = |I(-\Delta V, -B)|$, similar to that in EMCA [5,34], maintains.

The rest of the paper is organized as follows: In Sec. II, we provide a concise review of the theory employed in our study. In Sec. III, a general theory of nonreciprocal ballistic transport is elucidated. In Sec. IV, the physical results are specified in the two-dimensional (2D) Rashba gas subjected to an in-plane magnetic field. Finally, in Sec. V, we present our concluding remarks.

II. GAUGE-INVARIANT NONLINEAR QUANTUM TRANSPORT THEORY

Consider quantum coherent transport taking place in a mesoscopic system with connection to multiple terminals labeled by $\{\alpha\}$. The electric current I_α in terminal α driven by the bias voltages $\{\mathcal{V}_\alpha\}$ is expressed as [30,35–37]

$$I_\alpha = -\frac{e}{h}\sum_\beta \int d\mathrm{E}\mathrm{T}_{\alpha\beta}(E, U)(f_\alpha - f_\beta), \tag{1}$$

where $f_\alpha \equiv f(E - \mu_\alpha)$ is the Fermi-Dirac distribution function in terminal α, with $\mu_\alpha = E_F - e\mathcal{V}_\alpha$; E_F is the equilibrium Fermi energy; and $\mathcal{V}_\alpha$ is the bias voltage. The transmission from terminal β to terminal α is given by $T_{\alpha\beta} = \mathrm{Tr}[\Gamma_\alpha \mathcal{G}^r \Gamma_\beta \mathcal{G}^a]$, where $\mathcal{G}^{r(a)}$ is the retarded (advanced) Green's function defined as

$$\mathcal{G}^{r(a)}(E, U) = \frac{1}{E - H + eU - \Sigma^{r(a)}},$$
$$\Sigma^{r(a)} = \sum_\alpha \Sigma_\alpha^{r(a)}, \tag{2}$$

with $\Sigma_\alpha^{r(a)}$ being the retarded (advanced) self-energy introduced by terminal α that satisfies $\Sigma_\alpha^a = (\Sigma_\alpha^r)^\dagger$. The linewidth function is defined as $\Gamma_\alpha = i(\Sigma_\alpha^r - \Sigma_\alpha^a)$. For a two-terminal setup, the unitarity of the scattering matrix [38] ensures $T_{\mathrm{LR}} = T_{\mathrm{RL}}$.

In Eq. (2), H is the Hamiltonian of the system in equilibrium; i.e., all bias voltages vanish ($\mathcal{V}_\alpha = 0$). The additional term $U(x)$ is the Coulomb potential arising from a finite bias, which satisfies the Poisson equation [39]

$$\nabla^2 U(x) = 4\pi i e \int \frac{dE}{2\pi}[\mathcal{G}^<(E, U)]_{xx}, \tag{3}$$

where x denotes the position. The potential $U(x)$ plays an essential role for the nonreciprocal ballistic transport as the asymmetric band structures are considered. The lesser Green's function $\mathcal{G}^<$ is defined as $\mathcal{G}^< = \mathcal{G}^r \Sigma^< \mathcal{G}^a$, with

$$\Sigma^< = \sum_\alpha i\Gamma_\alpha f_\alpha. \tag{4}$$

In general, a self-consistent approach is required to solve Eqs. (2)–(4) in the nonlinear regime. Since the lesser Green's function exhibits a nonlinear relationship with U, Eq. (3) is a nonlinear differential equation. Nevertheless, the entire theoretical framework is gauge invariant [39], which means that the current is invariant under a uniform potential shift applied throughout the system.

Here, we focus on the weakly nonlinear regime, where the Coulomb potential can be expanded as

$$U(x) = \sum_\alpha u_\alpha(x)\mathcal{V}_\alpha + \cdots, \tag{5}$$

where the zeroth-order term (potential in equilibrium) has been absorbed into the Hamiltonian H, and $u_\alpha(x)$ denotes the characteristic potential [30,39]. Gauge invariance of the theory requires [30]

$$\sum_\alpha u_\alpha = 1. \tag{6}$$

To the lowest order, we derive the equation for $u_\alpha(x)$ from Eqs. (3) and (5) [30,40] as

$$-\nabla_x^2 u_\alpha + 4\pi e^2 \frac{dn}{dE} u_\alpha = 4\pi e^2 \frac{dn_\alpha}{dE}, \tag{7}$$

where $n(x)$ is the local charge density, and the injectivity or local partial density of states (LPDOS) of terminal α [30,40] is given by

$$\frac{dn_\alpha}{dE}(x) = \int \frac{dE}{2\pi}(-\partial_E f_0)\left[\mathcal{G}_0^r \Gamma_\alpha \mathcal{G}_0^a\right]_{xx}, \tag{8}$$

in which $\mathcal{G}_0^{r,a}$ is the equilibrium Green's function with $U(x) = 0$. An alternative expression for injectivity in terms of scattering wave functions and the velocity of incident modes

is [41,42]

$$\frac{dn_\alpha}{dE}(x) = \int \frac{dE}{2\pi}(-\partial_E f_0) \sum_n \frac{|\Psi_{\alpha n}(x)|^2}{\hbar |v_{\alpha n}|}, \tag{9}$$

where f_0 is the zero-bias distribution function, and $\Psi_{\alpha n}(x)$ and $v_{\alpha n}$ are the wave function and the velocity corresponding to the incident mode n from terminal α. The total injectivity contains the contributions from all terms as

$$\frac{dn}{dE}(x) = \sum_\alpha \frac{dn_\alpha}{dE}(x). \tag{10}$$

In the weakly nonlinear regime, we expand the current to the second order of the bias voltages as [30,31,39]

$$I_\alpha = \sum_\beta G_{\alpha\beta}\mathcal{V}_\beta + \sum_{\beta\gamma} G_{\alpha\beta\gamma}\mathcal{V}_\beta\mathcal{V}_\gamma + \cdots. \tag{11}$$

III. NONRECIPROCAL TRANSPORT IN THE BALLISTIC REGIME

In this section, we employ the theoretical framework introduced in the previous section to study nonreciprocal ballistic transport. We here focus on transport in a two-terminal setup. The current is assumed to flow in the x direction. The two terminals are situated on the left (L) and right (R) sides, with the corresponding biases denoted by $\mathcal{V}_\mathrm{L}$ and $\mathcal{V}_\mathrm{R}$, respectively. Due to the gauge invariance, the current flowing in two-terminal setups as formulated in Eq. (11) solely depends on the bias difference between the two terminals, which can be described by

$$I(\Delta V) = G_1\Delta V + G_2\Delta V^2 + O(\Delta V^3), \tag{12}$$

where $\Delta V = \mathcal{V}_\mathrm{L} - \mathcal{V}_\mathrm{R}$. For convenience, we set the bias configuration as $\mathcal{V}_\mathrm{L} = \mathcal{V}/2$ and $\mathcal{V}_\mathrm{R} = -\mathcal{V}/2$, corresponding to the voltage difference $\Delta V = \mathcal{V}$. Accordingly, the current in Eq. (1) reduces to

$$I(\mathcal{V}) = -\frac{e}{h}\int dE\, T[E, U(\mathcal{V})] \times \left[f\left(E - E_F + \frac{e\mathcal{V}}{2}\right) - f\left(E - E_F - \frac{e\mathcal{V}}{2}\right)\right]. \tag{13}$$

Without the bias-induced Coulomb potential, it is straightforward to prove the reciprocity of the transport, that is, $I(\mathcal{V}) = -I(-\mathcal{V})$. This conclusion fails as the bias-dependent Coulomb potential $U(\mathcal{V})$ is taken into account. Equation (5) now reduces to

$$U(\mathcal{V}) = (u_\mathrm{L} - u_\mathrm{R})\frac{\mathcal{V}}{2} + O(\mathcal{V}^2), \tag{14}$$

to the first order of $\mathcal{V}$. From Eq. (13), it is evident that if $T[E, U(\mathcal{V})] \neq T[E, U(-\mathcal{V})]$ then $|I(\mathcal{V})| \neq |I(-\mathcal{V})|$, giving rise to nonreciprocal ballistic transport. This can be achieved by $U(\mathcal{V}) \neq U(-\mathcal{V})$, or $u_\mathrm{L} \neq u_\mathrm{R}$ in Eq. (14). According to Eq. (7), this means that $dn_\mathrm{L}/dE \neq dn_\mathrm{R}/dE$. One way to achieve this condition is by breaking the translational symmetry along the transport direction using proper device geometries [30,43,44]. However, this strategy can readily drive the system away from the ballistic regime.

Here, we propose an alternative approach to realize nonreciprocal ballistic transport, taking advantage of the asymmetrical band structures with $E(k_x^\mathrm{L}) \neq E(k_x^\mathrm{R})$, where $k_x^{\mathrm{L,R}}$ are the wave vectors for the left- and right-moving states, respectively. The scenario is to lift the condition of $U(\mathcal{V}) = U(-\mathcal{V})$ by introducing unequal LPDOS in Eq. (9) for different terminals, which is achieved by the bias-resolved Coulomb potential. Specifically, for a given energy E, the opposite propagation states possess unequal velocities,

$$\left|v\left(k_x^\mathrm{L}, E\right)\right| \neq \left|v\left(k_x^\mathrm{R}, E\right)\right|, \tag{15}$$

due to the asymmetry of the bands. For a uniform system, the spatial distribution of the eigenstates $|\Psi_{\alpha n}(x)|$ is independent of x and so is the LPDOS dn_α/dE. Similarly, the Coulomb potential remains constant throughout the scattering region so that the characteristic potentials satisfy $\nabla_x^2 u_\alpha = 0$. The characteristic potentials are then expressed as

$$u_\alpha = \frac{dn_\alpha}{dE}\Big/\frac{dn}{dE}. \tag{16}$$

This result is consistent with the local neutral approximation [30,39,42], where the local charge density is assumed to be zero everywhere inside the system. Since the LPDOS is solely determined by the velocities in Eq. (9), the asymmetric band structures assign different values to the LPDOS for the two terminals with $dn_\mathrm{L}/dE \neq dn_\mathrm{R}/dE$, which further gives $u_\mathrm{L} \neq u_\mathrm{R}$.

The analysis above highlights the key scenario for the nonreciprocal ballistic transport in asymmetric bands. Next, we introduce $U_c \equiv U(\mathcal{V}) = -U(-\mathcal{V})$, drop the higher-order terms $O(\mathcal{V}^2)$ in Eq. (14), and denote the transmission for $+\mathcal{V}$ as $T_+ \equiv T_\mathrm{LR}(E, U_c)$ and that for $-\mathcal{V}$ as $T_- \equiv T_\mathrm{LR}(E, -U_c)$ for brevity. It is conceivable that the nonreciprocal condition $T_+ \neq T_-$ holds in general. Expanding Eq. (13) in the weak nonlinear regime yields

$$\begin{aligned} I(\mathcal{V}) &\approx \frac{e^2}{h}\int dE(-\partial_E f_0)\left[T_0\mathcal{V} + \frac{e}{2}(\partial_E T_0)(u_\mathrm{L} - u_\mathrm{R})\mathcal{V}^2\right] \\ &= G_1\mathcal{V} + G_2\mathcal{V}^2, \end{aligned} \tag{17}$$

where $T_0 \equiv T_\mathrm{LR}(E, U = 0)$, and the first-order and second-order conductances are expressed as

$$\begin{aligned} G_1 &= \frac{e^2}{h}\int dE(-\partial_E f_0)T_0, \\ G_2 &= \frac{e^3}{2h}(u_\mathrm{L} - u_\mathrm{R})\int dE(-\partial_E f_0)(\partial_E T_0). \end{aligned} \tag{18}$$

In the limit of zero temperature, the integration in Eq. (17) simplifies to

$$I \approx \frac{e^2}{h}\left[T_0\mathcal{V} + \frac{e}{2}(\partial_E T_0)(u_\mathrm{L} - u_\mathrm{R})\mathcal{V}^2\right], \tag{19}$$

where the energy is assumed to be at the Fermi energy E_F.

IV. NONRECIPROCAL BALLISTIC TRANSPORT IN RASHBA ELECTRON GAS

The scenario of nonreciprocal ballistic transport introduced in the previous section is general. Equation (17) indicates that

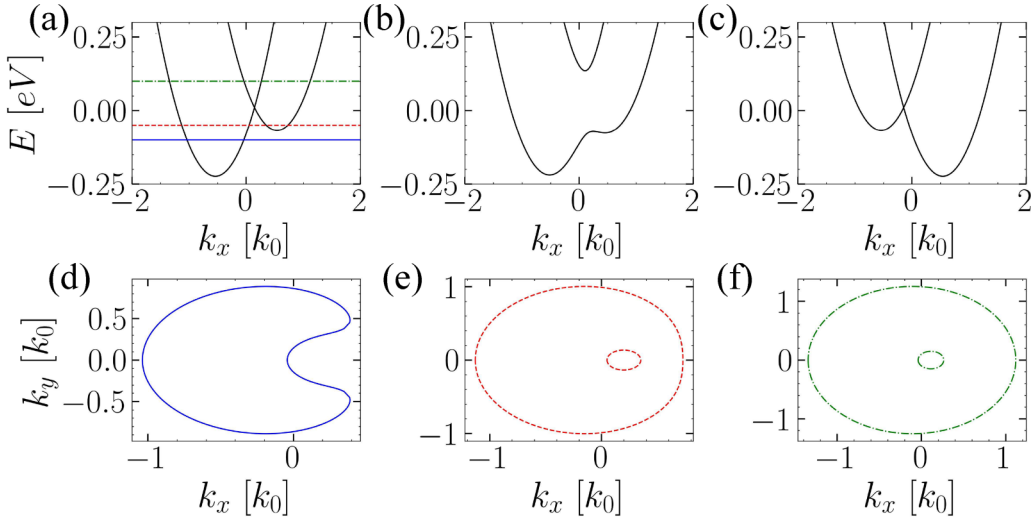

FIG. 2. The energy spectrum of the 2D SOC system, as calculated from Eq. (23), is illustrated in the following configurations. Panels (a) and (c) display the energy spectrum of the SOC system with $B_y = B_0$ and $-B_0$, respectively, at a fixed $k_y = 0$. Panel (b) shows the energy spectrum with $B_y = B_0$ and $k_y = 0.2k_0$. Panels (d)–(f) depict the Fermi surfaces, which are closed contours in the 2D system, at $E_F = -0.1$, -0.05, and 0.1 eV, corresponding to the levels shown in panel (a), with $B_y = B_0$. Here, the parameters are $m = 0.15m_e$, with m_e being the mass of a bare electron; $\lambda = 3.85$ eV Å [7]; k_0 satisfying $\hbar^2 k_0^2/m = 1$ eV; and $B_0 = 0.078$ eV.

a nonzero second-order conductance G_2 necessitates $u_L \neq u_R$ and $\partial_E T_0 \neq 0$. In quasi-1D systems, where transmission T_0 is quantized, achieving nonzero $\partial_E T_0$ is theoretically impossible. However, a continuous and differentiable $T_0(E)$—a prerequisite for nonzero $\partial_E T_0$—can be realized in 2D and 3D systems, as well as in quasi-1D systems with heterogeneous leads and the scattering region.

In this section, we elucidate the physical effects using the concrete example of 2D Rashba electron gas subjected to an in-plane magnetic field, which realizes asymmetric band structures. We investigate the modulation of the internal Coulomb potential induced by the bias voltages and the resultant nonreciprocal transport properties. The physical conditions for the implementation of the nonreciprocal transport are given.

A. 2D Rashba gas with asymmetric bands

We consider the 2D electron gas with Rashba spin-orbit coupling (SOC) subjected to an in-plane magnetic field, which can be captured by the Hamiltonian as

$$H(\mathbf{k}) = \frac{\hbar^2 k^2}{2m} + \lambda(k_x\sigma_y - k_y\sigma_x) - B_y\sigma_y, \tag{20}$$

where m denotes the effective electron mass, λ represents the strength of the SOC, $k^2 = k_x^2 + k_y^2$ defines the magnitude of the wave vector, and B_y is the Zeeman splitting induced by the in-plane magnetic field along the y axis.

When B_y is zero, the system satisfies both space-inversion symmetry (SIS) and time-reversal symmetry (TRS). Utilizing the QSYMM package [45], we identify the unitary symmetries related to SIS, including inversion symmetry with the action $\mathcal{S} = \sigma_z$, and mirror symmetries along the x and y directions with actions $\mathcal{M}_x = \sigma_x$ and $\mathcal{M}_y = i\sigma_y$, respectively. These symmetry operations transform the Hamiltonian as follows:

$$\begin{aligned} \mathcal{S}^\dagger H(\mathbf{k})\mathcal{S} &= H(-\mathbf{k}), \\ \mathcal{M}_x^\dagger H(k_x, k_y)\mathcal{M}_x &= H(-k_x, k_y), \\ \mathcal{M}_y^\dagger H(k_x, k_y)\mathcal{M}_y &= H(k_x, -k_y). \end{aligned} \tag{21}$$

TRS is represented as an antiunitary symmetry with the action $\mathcal{T} = \sigma_y\mathcal{K}$, where $\mathcal{K}$ is the complex conjugation operator, and it satisfies

$$\mathcal{T}^\dagger H(\mathbf{k})\mathcal{T} = H(-\mathbf{k}). \tag{22}$$

When B_y is nonzero, symmetries associated with $\mathcal{S}$, $\mathcal{M}_x$, and $\mathcal{T}$ are all broken, leading to an asymmetric band structure along the x direction (cf. Fig. 2). Specifically, the energy dispersions are

$$E_\pm(\mathbf{k}) = \frac{\hbar^2 k^2}{2m} \pm \sqrt{(\lambda k_x - B_y)^2 + \lambda^2 k_y^2}. \tag{23}$$

The x component of the velocities are

$$v_\pm^x = \frac{\hbar k_x}{m} \pm \frac{\lambda(\lambda k_x - B_y)}{\hbar\sqrt{(\lambda k_x - B_y)^2 + \lambda^2 k_y^2}}. \tag{24}$$

As our setup is infinite and translationally invariant along the y direction, we simplify our model by assuming the potential U to be independent of y. This assumption facilitates a simplified solution for the characteristic potential, analogous to the formulation presented in Eq. (16). The LPDOS contains the contribution from all k_y channels and can be expressed as

$$\frac{dn_\alpha}{dE} = \int \frac{dk_y}{2\pi}\frac{dn_{\alpha,k_y}}{dE}, \tag{25}$$

where $dn_{\alpha,k_y}/dE$ represents the LPDOS of the k_y channel in terminal α. In the ballistic limit, where k_x remains a good quantum number and the terminals share the same

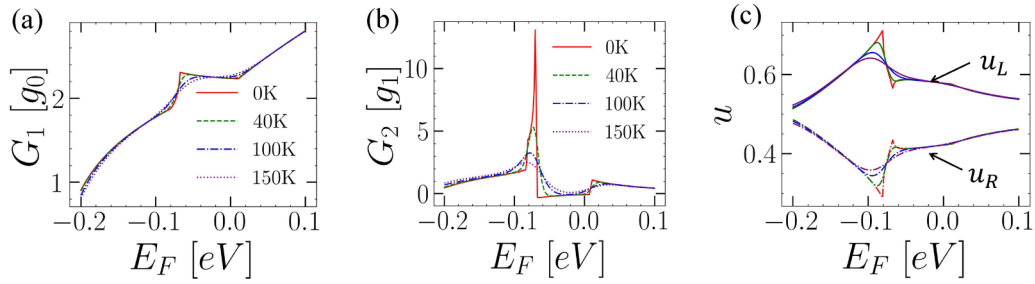

FIG. 3. Panels (a), (b), and (c) display the first-order conductances, the second-order conductances, and the characteristic potentials of the two terminals, respectively, at varying temperatures of 0, 40, 100, and 150 K. In these figures, $B_y = B_0$ is fixed, and the other system parameters are identical to those presented in Fig. 2. Specifically, in panel (c), the solid and dashed lines represent the characteristic potentials $u_{\rm L}$ and $u_{\rm R}$, respectively. These lines correspond to the same temperatures as those in panels (a) and (b), indicated by matching colors. The parameters g_0 and g_1 are defined such that $g_0 = \frac{e^2 L_y k_0}{2\pi h}$ and $\frac{g_0}{2g_1} = 1$ V.

Hamiltonian as the system, the total transmission is directly evaluated as

$$T_0 = \frac{L_y}{2\pi}\sum_{n=\pm}\int dk_x dk_y \theta\left(v_n^x\right) v_n^x \delta(E - E_n), \tag{26}$$

where L_y denotes the width of the scattering region in the y direction, and $\theta(\cdots)$ and $\delta(\cdots)$ are the Heaviside step function and the Dirac delta function, respectively. The LPDOS of the left and right terminals can be simplified as

$$\frac{dn_{\rm L,R}}{dE} = \frac{-1}{(2\pi)^2}\sum_{n=\pm}\int dk_x dk_y \theta\left(\pm v_n^x\right)\partial_{E_n} f(E_n - E_F), \tag{27}$$

where L and R correspond to $+v_n^x$ and $-v_n^x$, respectively. As the temperature approaches zero, $dn_{\rm L,R}/dE$ becomes proportional to the carrier density of the Fermi arcs for the left- and right-moving modes, as indicated by Eq. (27). When the Fermi surfaces (loops in the 2D case) are asymmetric, as shown in Figs. 2(d)–2(f), $dn_{\rm L}/dE \neq dn_{\rm R}/dE$. According to Eqs. (16) and (17), nonreciprocal transport phenomena can be expected.

B. Results and discussions

We start by analyzing the asymmetric energy bands described by Eq. (23), as depicted in Fig. 2. For a given energy in the k_y channel, the velocities of the counterpropagating states are unequal, like the density of states (DOS). Such band asymmetry necessitates the violation of SIS and TRS, which are symmetries $\mathcal{S}$, $\mathcal{M}_x$, and $\mathcal{T}$ here. Figures 2(d)–2(f) reveal the broken reflection symmetry of the Fermi loops about the k_x axis, which gives rise to different characteristic potentials $u_{\rm L}$ and $u_{\rm R}$ and leads to the emergence of second-order conductance G_2, as formulated in Eq. (18). In Fig. 3, we plot the characteristic potentials and two conductances $G_{1,2}$. The nonreciprocal transport is revealed by the second-order conductance G_2 in Fig. 3(b). According to Eq. (18), it is proportional to the difference of characteristic potentials $u_{\rm L} - u_{\rm R}$; see Fig. 3(c). From Fig. 3(b), one can see that the most pronounced nonreciprocal signals occur at $E_F \approx -0.07$ eV, when the Fermi energy coincides with the higher band bottom in Fig. 2(a). It is associated with the von Hove singularity in the DOS, resulting in a sudden alteration in conductance G_1, as depicted in Fig. 3(a), where the derivative of G_1 undergoes an abrupt change at $E_F \approx -0.07$ eV. This observation aligns with findings in the diffusive limit [7]. However, our results in the ballistic limit display persistent nonvanishing signals even when the Fermi energy is above the Dirac point, thus differentiating them from diffusive transport behaviors [7].

In Fig. 4, we illustrate how the conductances and the first-order potential are influenced by both the Fermi energy and the magnetic field B_y. When B_y is inverted to $-B_y$, the conductance G_1 remains unchanged, as does its derivative with respect to energy; see Fig. 4(a). Concurrently, the energy band structure reverses along the k_x direction, as shown in Figs. 2(a) and 2(c). This reversal swaps the characteristic potentials from $u_{\rm L(R)}$ to $u_{\rm R(L)}$, given that the LPDOS is fully determined by the band structures. This phenomenon is manifested in Fig. 4(c), where the first-order potential U is an odd function of B_y for a given E_F. As for Eq. (18), the conductance G_2 should also invert its sign, corresponding to the observation in Fig. 4(b). It is noted that the Onsager reciprocal relation [33] is violated,

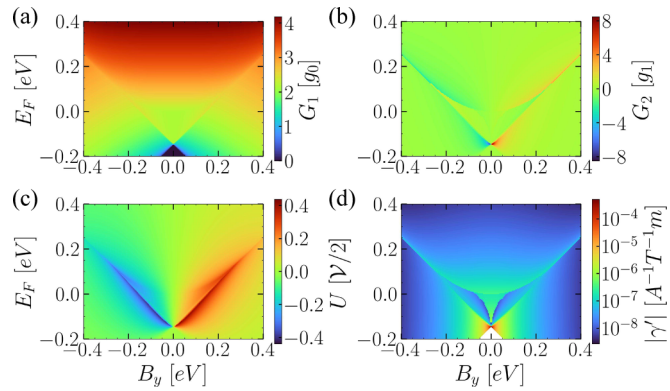

FIG. 4. Contour plot figures are presented to illustrate the following: (a) and (b) the first-order conductance G_1 and the second-order conductance G_2, as expressed in Eq. (18); (c) the first-order potential U, as expressed in Eq. (14); and (d) the magnitude of $\gamma' = \gamma L_y$, with γ defined in Eq. (28). They are in relation to variations in the Fermi energy and the Zeeman energy B_y. The parameters here are consistent with those used in Fig. 3, with the temperature fixed at 0 K. We take $g = 60$ as the g factor [7] to determine the magnetic field when calculating γ.

as $|I(\mathcal{V}, B)| \neq |I(-\mathcal{V}, B)|$. However, the relation $|I(\mathcal{V}, B)| = |I(-\mathcal{V}, -B)|$ holds, akin to the EMCA effects [5,6,34].

The resistance formula is commonly adopted in nonreciprocal transport measurements. The expression for resistance, as discussed in Refs. [5,34], can be obtained from Eq. (17) as

$$R = \frac{\mathcal{V}}{I} = R_0(1 - \gamma IB), \tag{28}$$

where

$$R_0 = \frac{1}{G_1}, \quad \gamma = \frac{G_2}{G_1^2 B}.$$

We plot $\gamma' = \gamma L_y$ as a function of B_y and E_F in Fig. 4(d). In the funnel-mouth-shaped region, where B_y is relatively small and the Fermi energy lies between the higher band bottom and the Dirac point, γ' appears to be largely independent of B_y. This result coincides with that in the diffusive limit [7]. However, it is noteworthy that the magnitude of γ' in this region, approximately 10^{-6} A^{-1} T^{-1} m, is significantly larger than that reported in Ref. [7].

V. CONCLUSIONS

In conclusion, our theoretical investigation focuses on nonreciprocal transport in energy band asymmetric systems within the quantum ballistic regime. A pivotal aspect of our study is the consideration of Coulomb potentials induced by finite biases. Antisymmetric biases at the left and right terminals lead to asymmetric potentials, a consequence of the inherent asymmetry in the band structure. Additionally, our analysis anticipates significantly larger nonreciprocal current signals in the quantum transport regime compared to diffusive bulk materials.

Furthermore, it is important to emphasize the wide applicability of the gauge-invariant weak nonlinear quantum transport theory to quantum nonreciprocal transport phenomena. This framework is versatile, extending to coherent nanoribbons and nanowires impacted by impurities and barriers, as well as to scenarios involving noncoherent transport. Specifically, our theoretical insights, particularly those derived from Eq. (17), offer qualitative understanding across a range of systems, leading to significant physical interpretations and conclusions. We hope that our work will provide valuable insights for future quantum transport experiments.

ACKNOWLEDGMENTS

This work was supported by the State Key Program for Basic Researches of China under Grant No. 2021YFA1400403 (D.Y.X.) and the National Natural Science Foundation of China under Grants No. 11974168 (L.S.), No. 12174182 (D.Y.X.), No. 12074172 (W.C.), No. 12222406 (W.C.), No. 12274235 (R.M.), and No. 12304068 (H. G.).

M.H.Z. and H.G. contributed equally to this work.

[1] Y. Tokura and N. Nagaosa, Nonreciprocal responses from non-centrosymmetric quantum materials, Nat. Commun. **9**, 3740 (2018).

[2] T. Ideue and Y. Iwasa, Symmetry breaking and nonlinear electric transport in van der Waals nanostructures, Annu. Rev. Condens. Matter Phys. **12**, 201 (2021).

[3] M. Fruchart, R. Hanai, P. B. Littlewood, and V. Vitelli, Non-reciprocal phase transitions, Nature (London) **592**, 363 (2021).

[4] T. Akamatsu, T. Ideue, L. Zhou, Y. Dong, S. Kitamura, M. Yoshii, D. Yang, M. Onga, Y. Nakagawa, K. Watanabe, T. Taniguchi, J. Laurienzo, J. Huang, Z. Ye, T. Morimoto, H. Yuan, and Y. Iwasa, A van der Waals interface that creates in-plane polarization and a spontaneous photovoltaic effect, Science **372**, 68 (2021).

[5] G. L. J. A. Rikken, J. Fölling, and P. Wyder, Electrical magnetochiral anisotropy, Phys. Rev. Lett. **87**, 236602 (2001).

[6] V. Krstić, S. Roth, M. Burghard, K. Kern, and G. L. J. A. Rikken, Magneto-chiral anisotropy in charge transport through single-walled carbon nanotubes, J. Chem. Phys. **117**, 11315 (2002).

[7] T. Ideue, K. Hamamoto, S. Koshikawa, M. Ezawa, S. Shimizu, Y. Kaneko, Y. Tokura, N. Nagaosa, and Y. Iwasa, Bulk rectification effect in a polar semiconductor, Nat. Phys. **13**, 578 (2017).

[8] Y. M. Itahashi, T. Ideue, Y. Saito, S. Shimizu, T. Ouchi, T. Nojima, and Y. Iwasa, Nonreciprocal transport in gate-induced polar superconductor $SrTiO_3$, Sci. Adv. **6**, eaay9120 (2020).

[9] Y. Li, Y. Li, P. Li, B. Fang, X. Yang, Y. Wen, D.-x. Zheng, C.-h. Zhang, X. He, A. Manchon, Z.-H. Cheng, and X.-x. Zhang, Nonreciprocal charge transport up to room temperature in bulk Rashba semiconductor α-GeTe, Nat. Commun. **12**, 540 (2021).

[10] C. O. Avci, K. Garello, A. Ghosh, M. Gabureac, S. F. Alvarado, and P. Gambardella, Unidirectional spin Hall magnetoresistance in ferromagnet/normal metal bilayers, Nat. Phys. **11**, 570 (2015).

[11] K. Yasuda, H. Yasuda, T. Liang, R. Yoshimi, A. Tsukazaki, K. S. Takahashi, N. Nagaosa, M. Kawasaki, and Y. Tokura, Nonreciprocal charge transport at topological insulator/superconductor interface, Nat. Commun. **10**, 2734 (2019).

[12] D. Choe, M.-J. Jin, S.-I. Kim, H.-J. Choi, J. Jo, I. Oh, J. Park, H. Jin, H. C. Koo, B.-C. Min, S. Hong, H.-W. Lee, S.-H. Baek, and J.-W. Yoo, Gate-tunable giant nonreciprocal charge transport in noncentrosymmetric oxide interfaces, Nat. Commun. **10**, 4510 (2019).

[13] S. Shim, M. Mehraeen, J. Sklenar, J. Oh, J. Gibbons, H. Saglam, A. Hoffmann, S. S.-L. Zhang, and N. Mason, Unidirectional magnetoresistance in antiferromagnet/heavy-metal bilayers, Phys. Rev. X **12**, 021069 (2022).

[14] C. Ye, X. Xie, W. Lv, K. Huang, A. J. Yang, S. Jiang, X. Liu, D. Zhu, X. Qiu, M. Tong, T. Zhou, C.-H. Hsu, G. Chang, H. Lin, P. Li, K. Yang, Z. Wang, T. Jiang, and X. Renshaw Wang, Nonreciprocal transport in a bilayer of $MnBi_2Te_4$ and Pt, Nano Lett. **22**, 1366 (2022).

[15] K. Yasuda, T. Morimoto, R. Yoshimi, M. Mogi, A. Tsukazaki, M. Kawamura, K. S. Takahashi, M. Kawasaki, N. Nagaosa, and Y. Tokura, Large non-reciprocal charge transport mediated by

quantum anomalous Hall edge states, Nat. Nanotechnol. **15**, 831 (2020).

[16] Z. Zhang, N. Wang, N. Cao, A. Wang, X. Zhou, K. Watanabe, T. Taniguchi, B. Yan, and W.-b. Gao, Controlled large nonreciprocal charge transport in an intrinsic magnetic topological insulator $MnBi_2Te_4$, Nat. Commun. **13**, 6191 (2022).

[17] H. Ishizuka and N. Nagaosa, Anomalous electrical magnetochiral effect by chiral spin-cluster scattering, Nat. Commun. **11**, 2986 (2020).

[18] K. Yasuda, A. Tsukazaki, R. Yoshimi, K. S. Takahashi, M. Kawasaki, and Y. Tokura, Large unidirectional magnetoresistance in a magnetic topological insulator, Phys. Rev. Lett. **117**, 127202 (2016).

[19] D. Kaplan, T. Holder, and B. Yan, Unification of nonlinear anomalous Hall effect and nonreciprocal magnetoresistance in metals by the quantum geometry, Phys. Rev. Lett. **132**, 026301 (2024).

[20] N. Wang, D. Kaplan, Z. Zhang, T. Holder, N. Cao, A. Wang, X. Zhou, F. Zhou, Z. Jiang, C. Zhang, S. Ru, H. Cai, K. Watanabe, T. Taniguchi, B. Yan, and W. Gao, Quantum-metric-induced nonlinear transport in a topological antiferromagnet, Nature (London) **621**, 487 (2023).

[21] M. Mehraeen, P. Shen, and S. S.-L. Zhang, Quantum unidirectional magnetoresistance, Phys. Rev. B **108**, 014411 (2023).

[22] H. Geng, J. Y. Wei, M. H. Zou, L. Sheng, W. Chen, and D. Y. Xing, Nonreciprocal charge and spin transport induced by non-Hermitian skin effect in mesoscopic heterojunctions, Phys. Rev. B **107**, 035306 (2023).

[23] K. Shao, H. Geng, E. Liu, J. L. Lado, W. Chen, and D. Y. Xing, A non-Hermitian moiré valley filter, arXiv:2310.10973.

[24] S. S.-L. Zhang and G. Vignale, Theory of unidirectional spin Hall magnetoresistance in heavy-metal/ferromagnetic-metal bilayers, Phys. Rev. B **94**, 140411(R) (2016).

[25] W. P. Sterk, D. Peerlings, and R. A. Duine, Magnon contribution to unidirectional spin Hall magnetoresistance in ferromagnetic-insulator/heavy-metal bilayers, Phys. Rev. B **99**, 064438 (2019).

[26] F. Freimuth, S. Blügel, and Y. Mokrousov, Theory of unidirectional magnetoresistance and nonlinear Hall effect, J. Phys.: Condens. Matter **34**, 055301 (2022).

[27] K. Kawabata and M. Ueda, Nonlinear Landauer formula: Nonlinear response theory of disordered and topological materials, Phys. Rev. B **106**, 205104 (2022).

[28] M. Büttiker, A. Prêtre, and H. Thomas, Dynamic conductance and the scattering matrix of small conductors, Phys. Rev. Lett. **70**, 4114 (1993).

[29] M. Büttiker, Charge and current conserving mesoscopic transport, in *Quantum Dynamics of Submicron Structures*, edited by H. A. Cerdeira, B. Kramer, and G. Schön (Springer, Dordrecht, 1995), pp. 657–672.

[30] T. Christen and M. Büttiker, Gauge-invariant nonlinear electric transport in mesoscopic conductors, Europhys. Lett. **35**, 523 (1996).

[31] M. Wei, B. Wang, Y. Yu, F. Xu, and J. Wang, Nonlinear Hall effect induced by internal Coulomb interaction and phase relaxation process in a four-terminal system with time-reversal symmetry, Phys. Rev. B **105**, 115411 (2022).

[32] M. Wei, L. Xiang, L. Wang, F. Xu, and J. Wang, Quantum third-order nonlinear Hall effect of a four-terminal device with time-reversal symmetry, Phys. Rev. B **106**, 035307 (2022).

[33] L. Onsager, Reciprocal relations in irreversible processes. I., Phys. Rev. **37**, 405 (1931).

[34] G. L. J. A. Rikken and P. Wyder, Magnetoelectric anisotropy in diffusive transport, Phys. Rev. Lett. **94**, 016601 (2005).

[35] A.-P. Jauho, N. S. Wingreen, and Y. Meir, Time-dependent transport in interacting and noninteracting resonant-tunneling systems, Phys. Rev. B **50**, 5528 (1994).

[36] M. P. Anantram and S. Datta, Effect of phase breaking on the ac response of mesoscopic systems, Phys. Rev. B **51**, 7632 (1995).

[37] S. Datta, *Quantum Transport: Atom to Transistor* (Cambridge University, Cambridge, England, 2005).

[38] H. Bruus and K. Flensberg, *Many-Body Quantum Theory in Condensed Matter Physics: An Introduction* (Oxford University, Oxford, 2004).

[39] B. Wang, J. Wang, and H. Guo, Nonlinear *I–V* characteristics of a mesoscopic conductor, J. Appl. Phys. **86**, 5094 (1999).

[40] M. Büttiker, Capacitance, admittance, and rectification properties of small conductors, J. Phys.: Condens. Matter **5**, 9361 (1993).

[41] J. Wang, Q. Zheng, and H. Guo, Weakly nonlinear quantum transport: An exactly solvable model, Phys. Rev. B **55**, 9763 (1997).

[42] B. Kramer, Editor, *Quantum Transport in Semiconductor Submicron Structures*, NATO Science Series E, Vol. 326 (Springer, Dordrecht, 2012).

[43] W.-D. Sheng, J. Wang, and H. Guo, Second-order non-linear conductance of a two-dimensional mesoscopic conductor, J. Phys.: Condens. Matter **10**, 5335 (1998).

[44] A. M. Song, A. Lorke, A. Kriele, J. P. Kotthaus, W. Wegscheider, and M. Bichler, Nonlinear electron transport in an asymmetric microjunction: A ballistic rectifier, Phys. Rev. Lett. **80**, 3831 (1998).

[45] D. Varjas, T. Ö. Rosdahl, and A. R. Akhmerov, Qsymm: Algorithmic symmetry finding and symmetric Hamiltonian generation, New J. Phys. **20**, 093026 (2018).